TOXICOLOGICAL SCIENCES **119(1)**, 135–145 (2011)
doi:10.1093/toxsci/kfq311
Advance Access publication October 7, 2010

Physicochemical Characterization and Ecotoxicological Assessment of CeO_2 Nanoparticles Using Two Aquatic Microorganisms

Ismael Rodea-Palomares,* Karina Boltes,† Francisca Fernández-Piñas,* Francisco Leganés,* Eloy García-Calvo,†,‡ Javier Santiago,† and Roberto Rosal†,‡,[1]

*Departamento de Biología, Facultad de Ciencias, Universidad Autónoma de Madrid, E-28049 Madrid, Spain; †Departamento de Ingeniería Química, Universidad de Alcalá, Alcalá de Henares, E-28871 Madrid, Spain; and ‡Advanced Study Institute of Madrid, IMDEA WATER, Parque Científico Tecnológico, Alcalá de Henres, 28805 Madrid, Spain

[1]To whom correspondence should be addressed. Fax: +34918855099. E-mail: roberto.rosal@uah.es.

Received July 28, 2010; accepted September 30, 2010

The physicochemical properties of nanoparticles determine their interaction with living organisms. Four different cerium oxide nanoparticles, including commercial materials, were characterized and compared with a micron-sized ceria. The formation of aggregates as well as ζ-potential, surface area, and chemical composition were determined. The formation of primary particle aggregates was a slow process that led to different particle sizes depending on the composition of the medium. In this paper, we describe the toxicity of cerium oxide for the self-luminescent cyanobacterial recombinant strain *Anabaena* CPB4337 and the green alga *Pseudokirchneriella subcapitata*. The toxicity for *Anabaena* exposed to nanoparticles in pure water for 24 h ranged from 0.27 to 6.3 mg/l; *P. subcapitata* EC_{50} (yielded effective concentration of nanoparticles that inhibits the cellular function of interest by 50%) values in the 2.4–29.6 mg/l range. Images of both organisms showed membrane disruption and highly damaged cells. Free cerium was highly toxic for both organisms, but the negligible amount found dissolved in the nanoparticle suspensions could not explain the observed toxic effect of nanoceria on the aquatic organisms; the dissolution of zinc could contribute to the toxicity of bulk material but could not explain the toxic effect of nanoceria either. We found no evidence of nanoparticle uptake by cells, but our observations suggested that their toxic mode of action required direct contact between nanoparticles and cells; in the case of the cyanobacterium, cells completely coated by layers of ceria nanoparticles were observed. Cell damage most probably took place by cell wall and membrane disruption; further research is needed to find out whether the oxidative activity of ceria could be responsible.

Key Words: **cerium oxide; microalgae; cyanobacteria; nanoparticles; membrane disruption.**

Nanosized particles have always been present in nature, but the accelerating penetration of engineered nanoparticles (ENP) in the market is raising serious concerns over their potential impact on the environment. A key aspect for the ecotoxicity assessment of ENP is the need to address their physicochemical behavior in biologically relevant media. This is because their environmental exposure is strongly dependent on adsorption and aggregation phenomena that may limit exposure but also promote locally high concentrations in sediments or biofilms (Handy *et al*., 2008). Cerium oxide nanoparticles have a wide range of applications. They are used as an additive in diesel fuel, but the commercial success of this application is limited; the main use of nanoceria being the formulation of slurries for the chemomechanical planarization (CMP) of silicon wafers in the production of integrated circuits.

Recent works have studied certain aspects of the effect of nano-CeO_2 in human cells. Xia *et al.* (2008) and Park *et al*., (2008b) studied their effect on bronchial epithelial cells (BEAS-2B) and found a toxic effect, which was related to the production of harmful reactive oxygen species (ROS). Both works demonstrated the effective uptake of nanoparticles by the cells. However, the toxicity of nanoceria is still not clear and Park *et al.* (2008a) reported, under the same conditions, the absence of any toxic effect in cell lines from the human brain and rat cardiomiocytes.

As far as ecologically relevant aquatic organisms are concerned, Roh *et al.* (2010) encountered a marked size-dependent effect of CeO_2 nanoparticles on the fertility and survival of the soil nematode *Caenorhabditis elegans*. Rogers *et al.* (2010) monitored the growth inhibition of *Pseudokirchneriella subcapitata* and assessed damage in cell membranes by measuring its permeability. They reported an effective concentration of nanoparticles that inhibits the cellular function of interest by 50% (EC_{50}) value of 10.3 mg/l of a 10- to 20-nm cerium oxide. Van Hoecke *et al.* (2009) found a significant chronic toxicity of three different-sized nanoceria for *P. subcapitata* and *Daphnia magna*, with EC_{50} for algal growth in the 7.6–28.8 mg/l range. Thill *et al.* (2006) and Zeyons *et al.* (2009) studied the toxicity of nano-CeO_2 for the bacteria *Synechocystis* PCC6803 and *Escherichia coli*. They reported close contact in the case of *E. coli* and nanoparticles, suggesting that toxicity could be because of an oxidative response associated with the reduction of Ce(IV) to Ce(III).

Fundamental questions regarding metal oxide nanoparticle toxicity remain unsolved. It is not clear whether the internalization of particles is relevant to the induction of intracellular effects or toxicity may be because of the adsorption of nanoparticles on the cellular membrane. This holds particularly for negatively charged particles because cell membranes possess large negatively charged domains, which should repel them. The question about the importance of particle size is still unanswered with very different toxic effects being reported for particles of similar size (Aruoja *et al*., 2009; Hartmann *et al*., 2010). Surface chemistry and the reason for toxic effects observed in non-nanoparticles are other points that require further attention and possibly a change in dose metrics, generally based on mass concentration.

The existing measurements of cerium oxide in the environment lead to exposure levels much lower than the estimated no effect dose for chronic human exposure (Park *et al*., 2008b). It has also been argued that exposure models predict concentrations significantly lower than those for which ecotoxicity investigations have encountered toxic effects. Therefore, most nanoparticles, in particular nanoceria, might not have any environmental impact (Tiede *et al*., 2009). Other data are more worrying. Limbach *et al*. (2008) have indicated that the majority of the nanoparticles are captured by clearing sludge in wastewater treatment plants, but up to 6 weight percentage of CeO_2 reaches the exit stream. On the other hand, although Registration, Evaluation, Authorization, and Restriction of Chemical substances regulation fails to consider the new risks posed by nanoparticles, the European Parliament recently published a report advocating extensive safety testing for manufactured nanomaterials.

The reason for choosing a green alga and a cyanobacterium was the ecological position of these organisms at the base of the aquatic food web and their essential role in nutrient cycling and oxygen production. Cyanobacteria constitute a phylum of bacteria that obtain their energy through plant-like photosynthesis. They are the most widespread primary producers at the base of the marine food chain and are also crucial in many other habitats including freshwaters, saline lakes, and biological soil crusts. Using different toxicity endpoints, this paper describes the toxic effect on these organisms of several nanoparticulate and micron-sized ceria, including commercially important samples. The physicochemical characterization of particles was extensive and helped to explain the observed toxicity for both organisms, as well as facilitating the integration of our data with previous or new research.

MATERIALS AND METHODS

Materials. In this work, we tested five different types of uncoated CeO_2 (CAS no. 1306-38-3) particles. The set included four types of nanoparticles with nominal primary particles in the 10–60 nm range and a micron-sized material (Sigma-Aldrich, powder, < 5000 nm, 99.9% trace metals basis) used as bulk reference (B5000). The nanoparticles included (1) Sigma-Aldrich cerium(IV) oxide nano powder, < 25 nm particle size (N25) either as powder or 5 weight percentage of suspension in water and (2) Sigma-Aldrich nano powder, < 50 nm particle size (N50), and two nanoceria provided by the Organization for Economic Cooperation and Development (OECD's) Working Party on Manufactured Nanomaterials. In accordance to their stated primary particle size, we referred to these two materials as N10 and N60. Both are commercial nanomaterials intended for use as an ingredient for diesel fuel and a component of CMP slurries, respectively. Cerium(III) chloride (CAS no. 7790-86-5) > 99.99% was purchased from Sigma-Aldrich. Water suspensions were prepared with high-purity water obtained from a Milipore Mili-Q system with a resistivity of at least 18 MΩ cm at 25°C. pH adjustments were made with analytical grade sodium hydroxide or hydrochloric acid from Merck. The reagents for OECD algal growth medium (AGM) and Allen and Armon modified medium were analytical grade reagents purchased from Sigma-Aldrich.

Characterization of nanoparticles. Concentrated suspensions of CeO_2 (100–160 mg/l) were prepared according to the following procedure. The prescribed amount of nanoparticle powder was mixed with a few drops of water in the bottom of a glass in order to create a paste. After a wetting period during which the paste was periodically removed, 50 ml of water or the liquid dispersing media was added. The glass was dispersed using a Sonics "VibraCell" ultrasound disperser (BioBlock Scientific, France) operating at 500 W for 30 s (90% amplitude). The procedure was agreed with other groups from OECD's Working Party on Manufactured Nanomaterials, and its purpose was to ensure a complete wetting and deagglomeration of the particulate solid. Once dispersion was completed, the deagglomerated suspension was taken to the desired volume according to the target final concentration and gently stirred with a magnetic rod for at least 2 h. Stock solutions were kept at 4°C in the dark and gently stirred before use or analysis while the temperature rose to normal room values.

Brunauer-Emmet-Teller surface area measurement and pore size distribution were determined by multipoint nitrogen adsorption at 77 K using a Beckman Coulter SA3100 device. Prior to analysis, samples were vacuum degassed at 200°C for 120 min. Chemical analysis was performed by Total Reflection X-ray Fluorescence (TXRF) using a Caneca 8030C spectrometer adjusted to obtain an excitation energy of 17.4 keV (Mo KR) and equipped with a Si(Li) detector (Oxford Instruments, U.K.). High-resolution transmission electron microscopy (TEM) images of nanoparticles were taken on a JEOL (JEM-2000 FX) microscope operating at 200 kV. TEM samples of nanoceria were prepared from 5 or 100 mg/l suspensions prepared as described previously. The size distribution of nanoparticles (< 6000 nm) was obtained using dynamic light scattering (DLS, Malvern Zetasizer Nano ZS). Zeta potential was measured via electrophoretic light scattering combined with phase analysis light scattering in the same instrument equipped with a Malvern autotitrator MPT-2. The measurements were conducted at 25°C using 10mM in KCl as the dispersing medium. Inductively Coupled Plasma—Mass Spectrometry analyses were performed on ultrafiltrated samples (10 kDa MWCO Vivaspin 6 Centrifugal Concentrator) on an Elan 6000 Perkin-Elmer Sciex device equipped with an autosampler AS 91. Cell counting was performed using a Z2 Coulter Counter Analyzer in line with International Standard (ISO 13319:2000).

Toxicity bioassays and analytical procedures. The toxicity of each suspension was determined by monitoring the growth inhibition of the green alga "*P. subcapitata*" and by determining the constitutive luminescence inhibition of the recombinant bioluminescent cyanobacterium *Anabaena* CPB4337. The final concentrations tested ranged from 0 (control samples) to 100 mg/l. The assays based on algal growth inhibition followed OECD TG 201. They were either performed in 96-well microplates, in which the algae were cultured in a total volume of 200 µl, or in 25-ml cultures conducted in 50-ml flasks mounted on a GFL 3005 orbital shaker. The growth of *P. subcapitata* was monitored daily for 72/96 h and assessed by optical density (OD) at 640 nm using a RAYTO RT-2100 C microplate reader and by direct cell counting using a Coulter Counter device (2.5–8.5 µm). Algae beads and culture media were

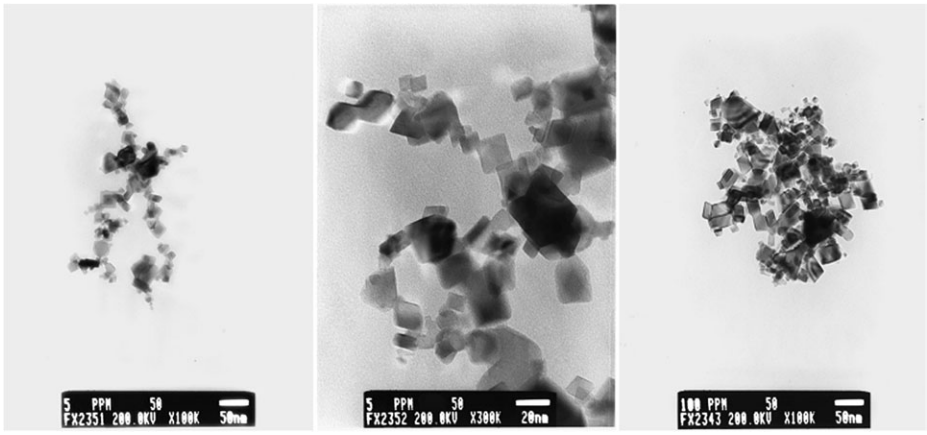

FIG. 1. TEM micrographs of suspensions of N50 particles in water at 5 mg/l (a and b) and 100 mg/l (c).

purchased from Microbiotest Inc. Microplates were maintained at 22°C inside a growing chamber with controlled light intensity (~100 µmol photons/m^2/s) and humidity levels, with no culture media evaporation and with periodical shaking and aeration. At least four replicates of each toxic concentration or blank were assayed using $ZnSO_4$ as standard for reproducibility control.

The bioassays using the bioluminescent cyanobacterium *Anabaena* CPB4337 were based on the inhibition of constitutive luminescence caused by the presence of toxics (Rodea-Palomares *et al*., 2009a,b). *Anabaena* CPB4337 was routinely at 28°C in the light, circa 65 µmol photons/m^2/s on a rotary shaker in 50 ml AA/8 medium supplemented with nitrate (5mM) in 125-ml Erlenmeyer flasks and 10 mg/ml of neomycin sulfate. The assays were conducted in 96-well microplates in a total volume of 200 µl. Bioassay details are given elsewhere (Rodea-Palomares *et al*., 2010). The assay media used were as follows: Mili-Q water, referred to as pure water (PW), pH 6; cyanobacterial culture medium AA/8 + N buffered with 2mM 4-(2-hydroxyethyl)-1-piperazineethanesulfonic acid (HEPES), pH 6; and AA/8 + N diluted 1/10 in Mili-Q water buffered with 2mM HEPES, pH 6 (denoted AA/8 + N and AA/8 + N 1/10, respectively). Luminescence was monitored 1, 4, and 24 h after exposure to the nanoparticle suspensions and cerium(III) chloride solutions.

Quantitative measurements of adenosine 5′-triphosphate (ATP) were performed as a direct biochemical indicator of toxicity using a BactTiter-Glo Microbial Cell Viability Assay (PROMEGA). The detection of ATP was based on the production of oxyluciferin whose signal was recorded using a Fluoroskan Ascent FL plate luminometer at spectral response 350–650 nm.

Bright-field micrographs were taken with an Olympus BH-2 microscope equipped with a Leica DC 300F digital camera. For TEM, cyanobacterial and algal cells exposed for different periods to increasing concentrations of the nanoparticle suspensions were collected by centrifugation, washed three times in phosphate buffer (0.1 M Na-phosphate, pH 7.2), and fixed in 3.1% glutaraldehyde made in phosphate buffer for 3 h at 4°C. Samples were washed three times and added to 4% bacteriological agar in phosphate buffer. Postfixation was on 1- to 2-mm agar blocks using osmium tetroxide in phosphate buffer for 2 h at 4°C. The samples were then dehydrated in ethanol and embedded in Durcupan resin (Fluka) sectioned in a Leica Reichert Ultracut S ultramicrotome, stained with uranyl acetate, and observed with a JEOL (JEM 1010) electron microscope at an operating voltage of 100 kV.

Statistical data treatment. The toxicity response of both organisms was estimated as EC_{50} and EC_{10}. We used EC_{10} as a surrogate for the no-observed effect concentration (Fox, 2008). For *Anabaena* CPB4337, these values were the effective concentration of toxicant that caused 50 or 10% bioluminescence inhibition with respect to a nontreated control. In *P. subcapitata*, they refer to the growth rate inhibition during the exponential growth phase. EC_x and their related statistical parameters such as standard deviation, coefficient of variation, and confidence intervals were estimated using a model-independent linear interpolation method (Norberg-King, 1993). The data were computed using software (inhibition concentration percentage [ICp]) freely available from Environmental Protection Agency statistical computer programs. ICp approach uses a nonparametric monotonic regression that does not depend on any particular model allowing point estimates and confidence intervals even without the entire dose-response curve.

RESULTS

Particle Characterization

The characterization of CeO_2 nanoparticles was performed using a combination of DLS, ζ-potential, TEM, total-reflection X-ray fluorescence (TXRF), and surface area measurement in order to provide clear insight into chemical composition, surface chemistry, particle size, and morphology. These properties are essential for a better understanding of nanoparticle toxicity for aquatic organisms.

A first essential property governing the behavior of nanoparticle suspension in aqueous media is their tendency to form aggregates or agglomerates. In what follows and in line with Rouquerol *et al*. (1994), the assemblage of primary particles will be denoted as "aggregate" because of their loose and unconsolidated character as shown by TEM. Figure 1 shows microphotographs of two samples of suspensions of N50 at two concentrations (5 and 100 mg/l). The images show the formation of loose structures at a low concentration that tend to become larger and more compact for higher loads. The powder morphology essentially consisted of truncated octahedrons with crystallite sizes considerably lower than the nominal 50-nm cutoff, with some specimens as small as a few nanometers. We never found small independent crystals in the TEM images. Pictures for the rest of the nanoceria samples are shown in supporting information (Supplementary figs. S1–3) and reveal a similar tendency to form aggregates of hundreds of nanometers. Only for the case of N10 was any different with particularly rounded primary particles which formed tighter aggregates, a morphology compatible with its

TABLE 1
Size of Aggregates (nanometer) of Suspensions of 100 mg/l of CeO_2 Measured by DLS in Pure Water at pH 6 after 24 h (PW + 24 h), Pure Water at pH 5 after 15 Days (PW + 15 Day), OECD AGM, pH 8, after 24 h (OECD AGM), and Allen and Arnon Modified Medium Diluted 1/10 and Adjusted to pH 6 in 2mM HEPES (AA8 + N 1/10)

	PW + 24 h	PW + 15 days	OECD AGM	AA/8 + N /10	AA/8 + N
$nCeO_2$-10	575	658	499	164	1081
$nCeO_2$-25	158	180	2107	155	2632
$nCeO_2$-50	218	235	1546	184	2285
$nCeO_2$-60	210	223	1599	185	2223
CeO_2-5000	195	283	417	199	1224

use as diesel fuel additive. The diffraction pattern obtained in TEM showed that all the samples were dominated by cerianite, the cubic form of CeO_2.

DLS confirmed that cerium oxide nano powders were always present as aggregates either in water or in algal and cyanobacterial culture media and that they could not be dispersed as primary particles. The aggregate formation was dynamic and took several hours to reach a stable size distribution. Supplementary figure S4 shows the result of monitoring a suspension of N50 for 1 week after preparation. DLS size distribution tends to become broader, and the particles, dispersed as explained in the previous section, still aggregated for some hours before reaching a suspension that was stable for weeks. Higher concentrations led to larger aggregates but always achieved a stable distribution within a few hours except for the case of N10 that aggregated for some days while approaching equilibrium (Supplementary fig. S5). In all cases, the suspension was stirred before analysis as indicated before. Table 1 shows representative results for the aggregate size measured by DLS in the nanometric region both in pure water and in the media used for bioassays. We found larger aggregates for AGM and concentrated Allen and Arnon modified medium. These differences may be because of the interaction of inorganic ions or other particles from the medium with the charged surface of nanoparticles as explained below. In pure water and diluted saline medium, the aggregates were in all cases below micron size. In all cases, the size of aggregates increased with the concentration of nanoparticles and, once prepared, tended to increase over time until achieving stable dispersion. The case of micron-sized ceria (B5000), nominally a bulk material, is particularly noteworthy. Both DLS and TEM pictures show that the dispersions contained a certain amount of primary nanoparticles, with aggregates not unlike from those found with nanoceria. TEM images show small crystallites, many of them below 20 nm, together with other small particles adhering to the larger ones (Supplementary fig. S6).

The tendency to form nanoparticle aggregates depends strongly on the surface charge. The particle charge, determined as ζ-potential by electrophoretic light scattering in a Malvern's ZetaSizer instrument, was negative in all cases (with values ranging from −12 to almost −30 mV) except for pure water, pH 6, where all nanoparticle suspensions gave a positive charge with relatively high positive values for N25 and N50. The isoelectric point, which corresponds to the pH at which the surface is neutral, was in the 6.0–7.5 region so that at the bioassay pH particle charge was low in all cases. We also determined that ζ-potential changed over time during the first few hours or days after preparing a suspension. Supplementary figure S7 in the supporting information shows the case of N50 measured just after preparation and 1 week later. After that time, we observed no further changes in any case. This effect can be explained by the adsorption of ions from solution or by the changes in the hydration state of the surface. ζ-Potential and isoelectric point are listed in Table 2.

The specific surface of all nanoparticle samples was in the 30–60 m^2/g range. The bulk oxide, however, had a much smaller surface (4.7 $m^2/g-$). Surface area characterization using nitrogen adsorption at 77 K also allowed the size of primary particles to be determined. The results are listed in Table 2. All materials exhibited a Type II isotherm (International Union of Pure and Applied Chemistry classification of adsorption isotherms) that corresponded to a macroporous adsorbent with strong adsorbate-adsorbent affinity. Supplementary figure S8 displays the full isotherm corresponding to N50. The pore volume for this material was 0.15 cm^3/g with 50% of pores between 15 and 50 nm (using Barrett-Joyner-Halenda desorption isotherm), the rest of the materials displaying similar characteristics. The chemical composition of samples assessed by TXRF detected calcium and very minor amounts of other metals, probably impurities from production precursors. Vanadium, chromium, manganese, iron, nickel, copper, gallium, arsenic, selenium, and bromine were below the detection limit in all samples. For the rest, the data are listed in Table 2. Worth noting is the fact that, in addition to cerium, we detected minor amount of metals including zinc, whose possible toxic effect is discussed below.

Ecotoxicity Results

The data shown in Table 3 correspond to the luminescence inhibition of *Anabaena* CPB4337 in water and in modified Allen and Armon medium (diluted up to one-tenth). The data include dissolved cerium chloride with doses expressed in milligrams per liter of Ce^{3+}. The results show a significant toxic effect for ceria nanoparticles duirng a 24-h assay in water at pH 6. Medium effect values were as low as 0.56 and 0.27 mg/l for N25 and N50, respectively. The toxicity of N25 and N50 in water is probably related to the positive ζ-potential measured in these conditions (Table 2). EC_{50} was also below 1 mg/l for dissolved Ce^{3+} and lower than 10 mg/l for the rest of

TABLE 2
Physicochemical Properties of Nanoparticulate and Bulk Cerium Oxide

	N10	N25	N50	N60	B5000
Size of primary particles (BET, nm)	12	13	22	28	176
BET surface area (m^2/g)	67.6	63.2	37.8	29.9	4.7
ζ-Potential (mV)					
Pure water, 10mM KCl, pH 8	−23.0 ± 1.7	−12.8 ± 0.5	−14.1 ± 0.4	−21.5 ± 1.1	−20.7 ± 2.3
Pure water, 10mM KCl, pH 6	+ 0.4 ± 0.8	+ 22.4 ± 1.3	+ 18.7 ± 0.8	+ 0.7 ± 1.1	+ 8.3 ± 0.9
AGM, pH 8	−12.5 ± 0.9	−15.5 ± 1.0	−16.0 ± 0.9	−10.9 ± 0.3	−12.2 ± 0.1
AA/8 + N 1/10, pH 6	−28.5 ± 1.2	−27.5 ± 1.1	−28.6 ± 0.8	−29.4 ± 1.4	−17.8 ± 0.7
AA/8 + N, pH 6	−26.9 ± 1.5	−19.5 ± 0.9	−20.3 ± 1.4	−15.6 ± 1.0	−16.2 ± 1.1
Isoelectric point (10mM KCl)	6.12	7.49	7.38	6.07	6.20
Chemical composition (TXRF, %)					
Cerium (as CeO_2)	91.2 ± 0.8	93.2 ± 1.1	97.7 ± 1.3	95.8 ± 1.4	90.8 ± 1.4
Calcium	5.20 ± 0.14	5.69 ± 0.18	1.49 ± 0.12	4.18 ± 0.24	7.45 ± 0.38
Titanium	1.11 ± 0.09	0.15 ± 0.10	< 0.083	nd	< 0.277
Zinc	0.018 ± 0.004	0.010 ± 0.006	0.021 ± 0.007	0.020 ± 0.010	0.014 ± 0.011
Sulfur	1.60 ± 0.35	0.93 ± 0.36	0.77 ± 0.39	< 1.236	1.03 ± 0.77
Chlorine	0.53 ± 0.20	< 0.333	< 0.234	< 0.449	< 0.856
Dissolved metals (10 kDa Ultrafiltrated, μg/l)					
Zinc	10.54 ± 0.07	9.15 ± 0.08	10.72 ± 0.07	14.89 ± 0.11	24.45 ± 0.12
Cerium	nd	nd	0.11 ± 0.06	nd	ns

Note. BET, Brunauer-Emmet-Teller; nd, not detected; ns, not significantly different from zero.

oxides including the bulk control. Table 3 also shows results in AA/8 + N 1/10 buffered at pH 6 with 2mM HEPES. The presence of salts considerably decreased the toxicity of particles but not that of dissolved cerium whose EC_{50} was 1.51 mg/l, the rest being above the highest assayed concentration; essentially, the same results were obtained when the undiluted medium, AA/8 + N, was used (not shown). Even without reaching EC_{50}, the toxic effect was apparent at very low concentrations in saline media. These results are given as EC_{10}. A certain hormetic effect, which appeared as the luminescence maximum in Table 3, was also observed during the first few hours.

The effect of CeO_2 particles and dissolved Ce^{3+} on the growth inhibition of *P. subcapitata* was assessed by measuring

TABLE 3
Dose-Effect Relationship Parameters for the Luminescence Inhibition Assays Using *Anabaena* CPB4337. EC_x in milligrams per liter of Particles or Dissolved Metal. The Boundaries Represent 95% Confidence Intervals. The Maximum Observed in AA/8 + N 1/10 Represents a Luminescence Transitory Enhancement

	1 h		4 h		24 h	
Pure water pH 6	EC_{50}	Boundaries	EC_{50}	Boundaries	EC_{50}	Boundaries
N10	69.4	56.9–77.0	33.7	25.9–39.8	6.3	4.7–8.5
N25	37.8	33.3–43.1	27.5	12.8–34.3	0.56	0.35–1.67
N50	44.9	41.4–49.8	46.6	32.0–71.8	0.27	0.20–0.58
N60	42.4	31.3–54.7	60.1	38.7–5.2	7.5	4.0–12.4
B5000	> 100	—	34.8	1.45–39.3	8.9	4.8–34.4
Ce^{3+}	> 100	—	> 100	—	0.78	0.08–3.69

	1–4 h		24 h		
AA/8 + N 1/10 HEPES 2mM pH 6	EC_{50}	Maximum (%)	EC_{50} and boundaries	EC_{10}	Boundaries
N10	> 100	+ 121	> 100	0.062	0.032–0.218
N25	> 100	+ 127	> 100	0.008	0.004–0.047
N50	> 100	+ 124	> 100	0.057	0.038–0.103
N60	> 100	+ 119	> 100	0.089	0.029–0.046
B5000	> 100	+ 117	> 100	0.021	0.003–0.030
Ce^{3+}	> 100	+ 121	1.51 (0.91±2.06)	0.003	0.002±0.007

TABLE 4
Dose-Effect Relationship Parameters for the Growth Rate of *Pseudokirchneriella subcapitata* Using Different Surrogates. EC_{50} in milligrams per liter of Particles or Dissolved Metal. The Growth Time Was 72 h Except for OD Readings in the Case of N10, N60, and B5000 for Which It Was Extended to 96 h

	OD		Cell counting		ATP	
	EC_{50}	Boundaries	EC_{50}	Boundaries	EC_{50}	Boundaries
N10	12.8	11.1–13.9	29.6	26.3–38.1	12.3	9.6–15.2
N25	0.95	0.88–1.02	9.7	8.5–11.5	5.2	3.2–7.4
N50	0.88	0.49–1.25	4.4	3.2–5.9	2.4	1.5–3.6
N60	8.96	8.20–9.72	16.4	13.6–19.9	8.5	5.6–11.7
B5000	16.5	15.4–17.7	56.7	45.9–67.9	20.3	16.5–24.4
Ce^{3+}	0.79	0.74–0.85	4.25	3.97–4.55	1.35	0.77–1.93

the OD of algae cultured in a microplate. The results, listed in Table 4, showed good reproducibility and indicated a high toxicity for dissolved cerium and two of the oxides (N25 and N50) and a relatively high effect for the rest, including the bulk ceria N5000. Both in microplate and in higher volume cultures, we observed a tendency for ceria particles to induce the flocculation of cells. Comparing EC_{50} values obtained from OD, with the growth rate obtained by direct cell counting, quantified this effect and allowed a direct surrogate to be obtained for biomass density. The results for microplate tests using direct cell counting are also listed in Table 4. A set of assays were also performed in 25-ml cultures in well-aerated shaken flasks with an initial cell load of 5×10^5 to 7×10^5 cells per milliliter. The results show considerably lower toxicity than that found in microplate cultures, with EC_{50} of 29.2 ± 3.0 mg/l for N50 and 35.7 ± 2.3 mg/l for N25, the boundaries representing 95% confidence intervals. Finally, the results obtained at 72 h using quantitative ATP detection show a higher toxic effect than that observed using daily cell counting, the highest toxicity corresponding to the dissolved Ce^{3+}.

The toxicity for the green alga assessed either by cell counting or by quantitative ATP measurement yields the same order of toxicity, ranging from the most toxic N50 to the micron-sized particles: N50 > N25 > N60 > N10 > B5000. The order of toxicity was almost the same as that found for *Anabaena* with N50 being the most toxic nanoparticle for both organisms.

In order to explore further the cellular mechanisms of the observed nanoparticle toxicity, we took both bright-field and TEM micrographs in pure water, pH 6, bioassay of *Anabaena*

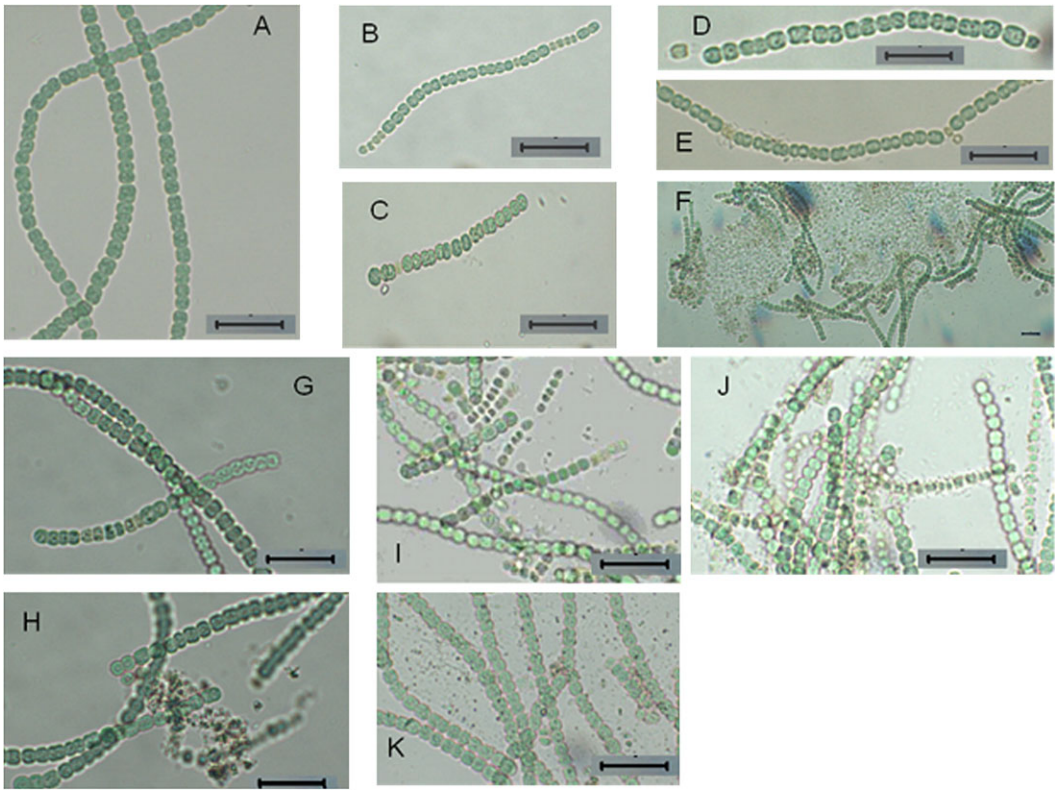

FIG. 2. Bright-field micrographs of *Anabaena* CPB4337 exposed to increasing concentrations of ceria nanoparticles. (A) Control *Anabaena* filaments. (B and C) *Anabaena* filaments exposed to 1 mg/l N10 for 48 h and 80 mg/l N10 for 72 h. (D, E, and F) *Anabaena* filaments exposed to 0.1 mg/l N25 for 72 h, 1 mg/l N25 for 24 h, and 80 mg/l for 24 h. (G and H) *Anabaena* filaments exposed to 0.01 mg/l N50 for 48 h and 50 mg/l N50 for 48 h. (I, J, and K) *Anabaena* filaments exposed to 1 mg/l N60 for 24 h, 50 mg/l N60 for 72 h, and 80 mg/l N60 for 24 h. Bars, 20 μm.

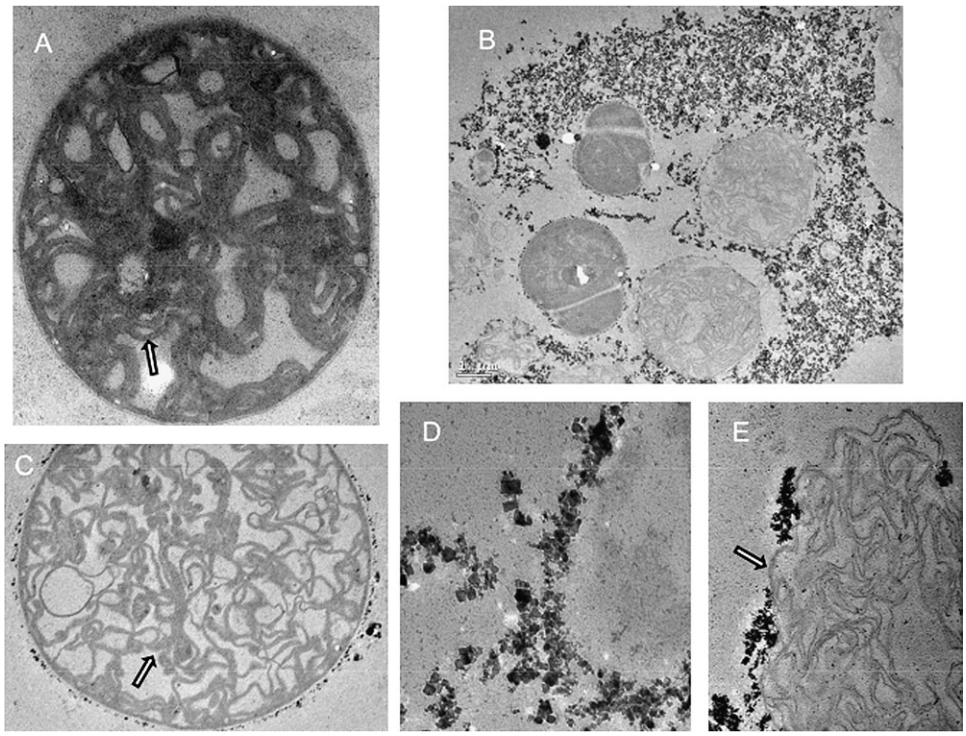

FIG. 3. TEM micrographs of *Anabaena* CPB4337 exposed to 80 mg/l N25 ceria nanoparticles for 24 h. (A) Control cell. (B) *Anabaena* cells in close contact to N25 aggregates. (C) *Anabaena* cell coated with N25 nanoparticles. (D) Detail of a highly damaged *Anabaena* cell coated with nanoceria showing the crystalline nature of the nanoparticles. (E) *Anabaena* cell that has lost cell envelopes with nanoparticle clusters attached to the thylakoids. Arrows indicate thylakoids. Bars: 0.5 μm (A), 1.0 μm (B), 1.0 μm (C), 0.1 μm (D), and 0.2 μm (E).

and *P. subcapitata* cells in AGM exposed to nanoparticle suspensions. Figure 2 shows that nanoparticle exposure generally resulted in a shortening and narrowing of *Anabaena* filaments, many of which manifested lysed or highly damaged cells; cell damage was already evident at low concentrations (0.01 and 0.1 mg/l, Fig. 2D, N25 and Fig. 2G, N50) of the most toxic nanoparticles, N25 and N50; for N10 and N60, damage to filaments and cells could be seen clearly at the higher concentration of 1 mg/l (Fig. 2B, N10 and Fig. 2I, N60). At high concentrations of most tested nanoparticles (Fig. 2F, N25; Fig. 2H, N50; and Fig. 2K, N60), what seemed to be large aggregates of nanoparticles could be seen. The filaments in contact with these aggregates were particularly damaged, and cell lysis debris was evident; curiously, at these high concentrations, apparently healthy filaments, which were not in direct contact with these large aggregates, could be found (e.g., filaments outside the large cell debris-nanoparticle aggregates in Fig. 2F). These observations suggest that direct contact between the nanoparticles/nanoparticle aggregates and cells could be relevant to the observed toxicity. In this regard, TEM images revealed cell damage whenever cells came into close contact with the nanoparticles; a clear example of this is Figure 3, which shows images at different magnifications of cells surrounded by large aggregates of N25 nanoparticles at 80 mg/l after 24 h of exposure. Figure 3C shows clearly an *Anabaena* cell whose cellular surface is completely coated by what seems to be a layer of nanoparticles; the crystalline structure of the nanoparticle coating is clearly visible in Figure 3D where layers of these nanoparticles cover the whole cell. The next micrograph (E) shows the remainder of a cell that has completely lost its cell wall and membrane; the nanoparticles aggregated and attached tightly to the cytoplasmatic photosynthetic membranes of cyanobacteria, the thylakoids. The observed strong adsorption of the nanoparticles to the cell wall may impair the surface architecture resulting in the complete disruption of the cell wall and membrane and leaving loose photosynthetic membranes where nanoparticles also attached themselves. Such strong adsorption followed by membrane disruption is most probably the cause of the observed toxicity that leads to cell lysis; Also, it is highly likely that when cells are completely trapped inside the shell of CeO_2 nanoparticles as in Figures 3C and 3D, nutrient transport is severely impaired with a resultant lack of essential nutrients and energy. As ceria nanoparticles are positively charged in the water bioassay medium and the cyanobacterial surface is negatively charged under these conditions, electrostatic attraction favors the observed strong adsorption of nanoparticles onto the cell surface that subsequently triggers cell damage.

The optical microphotographs for the green alga exposed to ceria (Fig. 4) show clearly the formation of particle aggregates that include algal cells. Figure 4B, which corresponds to a culture exposed to 40 mg/l N50 after 72 h, plainly shows how

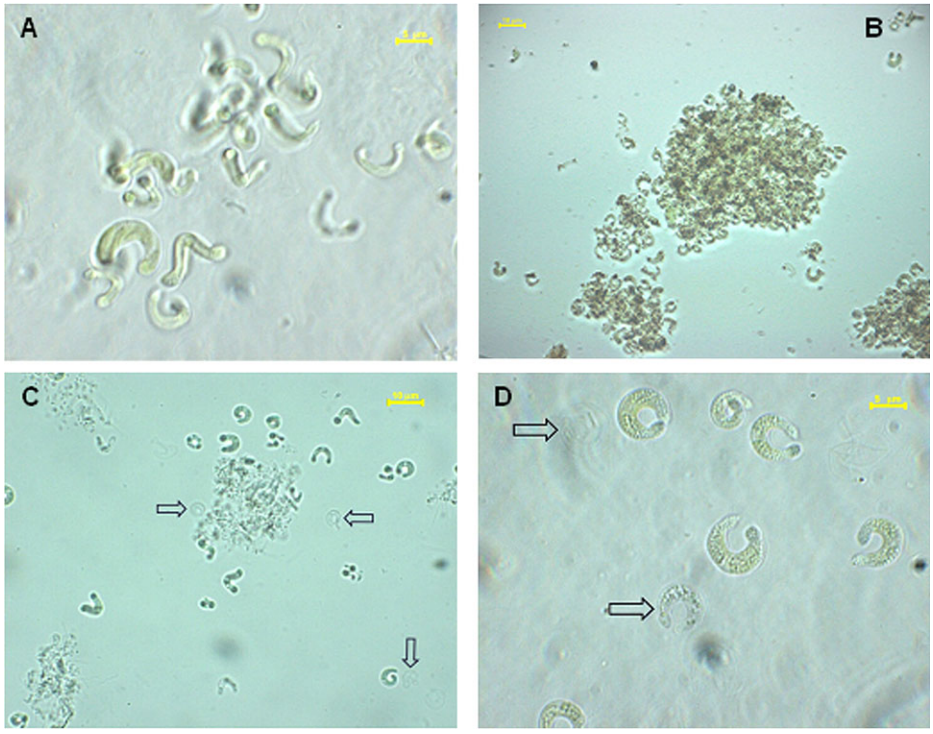

FIG. 4. Bright-field micrographs of *Pseudokirchneriella subcapitata* exposed to N50. (A) Control *Anabaena* filaments. (B) Algae exposed to 40 mg/l N50 for 72 h. (C) Algae exposed to 5 mg/l N50 for 48 h. (D) Cells exposed to 5 mg/l N50 for 72 h. Arrows indicate highly damaged cells. Bars: 5 μm (A), 10 μm (B), 5 μm (C), and 10 μm (D).

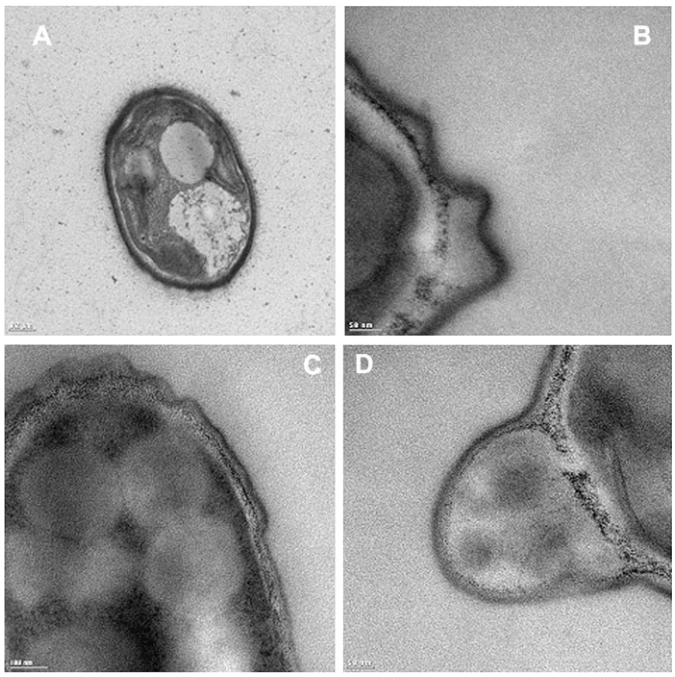

FIG. 5. TEM micrographs of *Pseudokirchneriella subcapitata* exposed to N50. (A) Control cells. (B, C, and D) Algae in contact with 2 mg/l for 48 h. Bars: 0.2 μm (A), 50 nm (B), 100 nm (C), and 50 nm (D).

particles and cells come into close contact even though particles at the bioassay pH are negatively charged as indicated in Table 2. For lower particle concentrations, the aggregates were looser, this is to say with a more extended conformation, but also contained cells in close contact with particles as shown in Figure 4C, which corresponds to a culture exposed for 48 h to 5 mg/l of N50. In this case, it can also be seen how aggregates coexisted with free cells that showed no apparent damage. Inside the looser aggregates and in the vicinity of many others, colorless cells could be seen quite clearly, which suggests damage to their internal structure. Figure 4D, taken at higher magnification after algae were kept during 72 h in contact with 5 mg/l N50, shows almost transparent cells that contrast sharply with the dark green ones whose chloroplast is easy to see. As far as TEM micrographs shown in Figure 5 are concerned, the occurrence of highly damaged cells, which otherwise coexisted with other apparently normal or with a minor degree of harm, may be observed. The TEM images of algae exposed to nanoceria plainly show damage to cell membranes. The disrupted cell wall appeared separated from the cell membrane with cytoplasm leaking into the vacuity (Figs. 5B and 5D). We further observed a parallel profusion of cytoplasmic vesicles, whereas chloroplast and the rest of the cell structures disappeared or became highly damaged (Fig. 5C). These highly damaged cells are supposed to

correspond to those that appeared as empty or transparent in bright-field images (Fig. 4D). Neither in the cyanobacterium nor in the alga did we find any evidence of nanoparticle uptake and internalization by cells.

DISCUSSION

The aggregation of metal oxides in water depends on particle charge and has a significant effect on their bioavailability. We have showed that cerium oxide nano powders form aggregates in water, taking a few hours or days to reach stable size distribution (Supplementary fig. S4). This is probably a consequence of the hydration of surface and the adsorption of ions from solution, both of them processes that reach equilibrium slowly. Nanoceria exhibited a certain decrease in ζ-potential during the first few hours or days after being put in suspension. Subsequent changes were negligible, and bulk oxide was observed to behave similarly. Berg *et al.* (2009) have reported a change in ζ-potential for nanoceria samples during the first few days after suspension. We found the largest aggregates in AGM and undiluted AA8 + N, most of them in the micron-sized region, the rest being mostly around 200 nm (Table 1). These differences should be because of the interaction of inorganic ions or particles from the medium with the surface of ceria. For the bulk material B5000, a clear peak in the few hundred nanometers was obtained in all cases according to the TEM images.

The detection of zinc by TXRF was significant because of its toxicity and ability to dissolve (Aruoja *et al.*, 2009). Franklin *et al.* (2007) have reported that EC_{50} was near 60 μg/l for the growth inhibition of *P. subcapitata*, whereas Rodea-Palomares *et al.*, (2009b) have reported EC_{50} values of dissolved zinc of 90 μg/l (1 h) and 79 μg/l (24 h) for *Anabaena* CPB4337. If all the zinc in the samples dissolved, the final concentration would be about 0.20 μg Zn^{2+}/mg CeO_2. We found a maximum concentration of 24 μg/l zinc for a suspension of 100 ppm (B5000). This would represent an amount of zinc of 2–13 μg/l at their EC_{50}, and consequently, the contribution of dissolved zinc to bulk oxide toxicity was not negligible. For the most toxic nanoceria, N25 and N50, the dissolution of all zinc in samples would yield a concentration of just 0.4–1.0 μg/l Zn^{2+} at their EC_{50}, and consequently, zinc dissolution cannot explain the observed toxicity in this case. The dissolution of ceria was negligible in all cases (Table 2).

Despite their role as primary producers in aquatic ecosystems, the toxicity of nanoparticles for cyanobacteria has only seldom been explored. Recently, Zeyons *et al.* (2009) have studied the effect of ceria nanoparticles on the unicellular cyanobacterium *Synechocystis* PCC6803 and observed a decrease of cell viability only at low concentrations of nanoparticles and in ultrapure water, but not in a synthetic salt medium. Our results (Table 3) show the clear toxicity of all tested ceria nanoparticles for the filamentous cyanobacterium *Anabaena* CPB4337. The effect was much more significant in the pure water assay at pH 6 than in the growth medium. As already mentioned, the presence of salts considerably decreased the toxicity of the particles. This could be the consequence of an aggregation effect because of the presence of other particles and dissolved electrolytes. However, the fact that toxicity also decreased in saline medium for dissolved cerium seems to indicate that the cells were inherently less vulnerable in the presence of salts. The fact that microorganisms are more susceptible to the toxic effect of nanoceria in salt-depleted media has also been reported by Thill *et al.* (2006) and Zeyons *et al.* (2009) who attribute it to the aggregation of nanoparticles in high–ionic strength media. It has been pointed out how, as ionic strength increases, the nanoparticle charge is neutralized more effectively (Keller *et al.*, 2010).

EC_{50} values for the green alga were in the range of those reported by Rogers *et al.* (2010) and Van Hoecke *et al.* (2009). Cell counting led to EC_{50} values approximately twice those obtained from ATP determinations, probably as a consequence of the lower ATP content of cells exposed to nanoparticles, an effect already described by Mortimer *et al.* (2010). The effect observed on the growth rate of *P. subcapitata* when using OD as surrogate was particularly high for the most toxic nanoparticles, N25 and N50. In this case, the suspensions showed a marked tendency to form aggregates and flocculate, an effect that was plain to see in larger volume cultures after shaking ceased. These low EC_{50} values reflect the clarification because of the formation of aggregates and are mainly a consequence of the physical effect of nanoparticles on cells.

To gain further insights into the way nanoparticles act, we studied the effect of ceria nanoparticles on the integrity of the cells. Optical micrographs of *Anabaena* CPB4337 exposed to ceria showed shortened and yellowed filaments with a significant percentage of highly damaged/lysed cells (Fig. 2). At higher nanoparticle concentrations, cell toxicity was clearly related to the presence of nanoparticle aggregates, with damaged cells concentrating in the neighborhood or adhering to the aggregates. As shown in Figure 3, we observed a high load of nanoparticles attached as a layer to the cell walls; this adsorption was most probably driven by the electrostatic attraction between the positively charged nanoparticles in the water assay and the negatively charged cell wall of the cyanobacterium. At higher magnifications, the crystalline nature of the nanoparticles coating the cells could be seen. Strong adsorption of ceria nanoparticles to cell walls has also been found for *E. coli* (Thill *et al.*, 2006; Zeyons *et al.*, 2009) and biological sludge (Limbach *et al.*, 2008); however, Zeyons *et al.* (2009) found no toxicity for the unicellular cyanobacterium *Synechocystis* but attributed it to the production of cyanobacterial exopolymeric substance (EPS), which may adsorb nanoparticles thus preventing their interaction with cell walls. *Anabaena* CPB4337 is a planktonic organism that does not produce EPS (Pereira *et al.*, 2009); this explains why ceria nanoparticles attach so strongly to it.

Van Hoecke *et al.* (2009) found no evidence of either the uptake/strong adsorption of CeO_2 nanoparticles to *P. subcapitata* or ultrastructural damage. However, although we found no evidence of particles anchored to the algal cell surface, we did observe membrane rupture, cytoplasm leakage, and intracellular damage (Figs. 5B, 5C, and 5D), all of which suggested direct contact between nanoparticles and algal cell envelopes. In this regard, the formation of aggregates between particles that included algal cells in close contact was plain to see (Figs. 4B and 4C). This aggregation effect was evidenced in the tendency to flocculate cells exposed to particle suspensions and could be a consequence of the alteration of the particle charge because of the release of cell material. As for the interaction of cells with negatively charged particles, Wilhelm *et al.* (2003) have suggested that these particles bind cationic sites on the cell surface to form clusters favored by the repulsive interactions with negatively charged domains. Once bound to the cell, these nanoparticles have a lower charge density that favors the adsorption of other particles and the formation of large clusters.

There could be several explanations of how attached nanoparticles exert toxicity on the cyanobacterial/algal cell; in the case of highly damaged *Anabaena* cells trapped inside the nanoparticle shell (Fig. 3D), the transport of nutrients and metabolites across cell wall and membrane could be affected, leading to cell death because of prolonged starvation as also pointed out by Zeyons *et al.* (2009) for *E. coli* cells tightly coated by ceria nanoparticles. In addition, tightly attached nanoparticles may cause mechanical damage to the cell membrane because of the numerous edges, corners, and reactive sites present in the crystal structure of the nanoparticle as suggested by Rogers *et al.* (2010). In the end, this mechanical damage may result in membrane disruption as we have found in both the optical and the TEM images of both organisms; alternatively, direct interaction between nanoparticles and the cell membrane may potentially generate ROS, thus inducing oxidative stress and cell toxicity. Thill *et al.* (2006) and Zeyons *et al.* (2009) have found a reduction of cerium(IV) to cerium(III) when the ceria nanoparticles were firmly adsorbed onto the outer membrane of *E. coli* and have linked it to a strong cytotoxicity that could be because of lipid/protein oxidation; in mammalian cells (Park *et al.*, 2008b), the cell toxicity of ceria nanoparticles was also linked to oxidative stress.

As indicated by our results and those of others (Rogers *et al.*, 2010; Thill *et al.*, 2006; Zeyons *et al.*, 2009), the direct contact of the ceria nanoparticles with the cell wall/membranes is essential for cytotoxicity to occur. The mechanisms underlying nanoceria toxicity seem to be mediated by direct contact with nanoparticles, thus resulting in cell wall and membrane disruption, which ultimately leads to cell lysis. It would be interesting to investigate whether nutrient transport is impaired in the nanoparticle-coated *Anabaena* cells and whether oxidative stress plays a role in membrane disruption and cytotoxicity, with special emphasis on the effect of nanoceria in photosynthesis, the main bioenergetic process of both organisms, which could also be involved in the generation of ROS when photosynthetic reactions are not well balanced. As far as dose metrics are concerned, our data did not support the view that surface area might work better than mass concentration as a dose variable.

SUPPLEMENTARY DATA

Supplementary data are available online at http://toxsci.oxfordjournals.org/.

FUNDING

Spanish Ministry of Education (grant CSD2006-00044); Spanish Ministry of Science and Innovation (grant CGL2010-15675, sub-programme BOS); Comunidad de Madrid (grants 0505/AMB-0395, 0505/MB/0321, S-2009/AMB/1511-Microambiente-CM).

ACKNOWLEDGMENTS

One of the authors, J.S., would like to thank the Spanish Ministry of Science for the award of a Formación de Profesorado Unviersitario grant.

REFERENCES

Aruoja, V., Dubourguier, H. C., Kasemets, K., and Kahru, A. (2009). Toxicity of nanoparticles of CuO, ZnO and TiO_2 to microalgae Pseudokirchneriella subcapitata. *Sci. Total Environ.* **407,** 1461–1468.

Berg, J. M., Romoser, A., Banerjee, N., Zebda, R., and Sayes, C. M. (2009). The relationship between pH and zeta potential of ~30 nm metal oxide nanoparticle suspensions relevant to *in vitro* toxicological evaluations. *Nanotoxicology* **3,** 276–283.

Fox, D. R. (2008). NECS, NOECS and the EC_x. *Australas. J. Ecotoxicol.* **14,** 7–9.

Franklin, N. M., Rogers, N. J., Apte, S. C., Batley, G. E., Gadd, G. E., and Casey, P. S. (2007). Comparative toxicity of nanoparticulate ZnO, bulk ZnO, and $ZnCl_2$ to a freshwater microalga (*Pseudokirchneriella subcapitata*): the importance of particle solubility. *Environ. Sci. Technol.* **41,** 8484–8490.

Handy, R. D., Owen, R., and Valsami-Jones, E. (2008). The ecotoxicology of nanoparticles and nanomaterials: current status, knowledge gaps, challenges, and future needs. *Ecotoxicology* **17,** 315–325.

Hartmann, N. B., Von der Kammer, F., Hofmann, T., Baalousha, M., Ottofuelling, S., and Baun, A. (2010). Algal testing of titanium dioxide nanoparticles—testing considerations, inhibitory effects and modification of cadmium bioavailability. *Toxicology* **269,** 190–197.

Keller, A. A., Wang, H., Zhou, D., Lenihan, H. S., Cherr, G., Cardinale, B. J., Miller, R., and Ji, Z. (2010). Stability and aggregation of metal oxide nanoparticles in natural aqueous matrices. *Environ. Sci. Technol.* **44,** 1962–1967.

Limbach, L. K., Bereiter, R., Müller, E., Krebs, R., Gälli, R., and Stark, W. (2008). Removal of oxide nanoparticles in a model wastewater treatment plant: influence of agglomeration and surfactants on clearing efficiency. *Environ. Sci. Technol.* **42,** 5828–5833.

Mortimer, M., Kasemets, K., and Kahru, A. (2010). Toxicity of ZnO and CuO nanoparticles to ciliated protozoa *Tetrahymena thermophila*. *Toxicology* **269,** 182–189.

Norberg-King, T. J. (1993). A Linear Interpolation Method for Sublethal Toxicity: The Inhibition Concentration (ICp) Approach Program and User Manual, Version 2.0. National Effluent Toxicity Assessment Center Technical Report 03–93. U.S. Environmental Protection Agency Environmental Research Laboratory, Duluth, MN.

Park, B., Donaldson, K., Duffin, R., Tran, L., Kelly, F., Mudway, I., Morin, J. P., Guest, R., Jenkinson, P., Samaras, Z., *et al*. (2008a). Hazard and risk assessment of a nanoparticulate cerium oxide-based diesel fuel additive—a case study. *Inhal. Toxicol.* **20,** 547–566.

Park, E. J., Choi, J., Park, Y. K., and Park, K. (2008b). Oxidative stress induced by cerium oxide nanoparticles in cultured BEAS-2B cells. *Toxicology* **245,** 90–100.

Pereira, S., Zille, A., Micheletti, E., Moradas-Ferreira, P., De Philippis, R., and Tamagnini, P. (2009). Complexity of cyanobacterial exopolysaccharides; composition, structure, inducing factors and putative genes involved in their biosynthesis and assembly. *FEMS Microbiol. Rev.* **33,** 917–941.

Rodea-Palomares, I., Fernández-Piñas, F., González-García, C., and Leganés, F. (2009a). Use of *lux*-marked cyanobacterial bioreporters for assessment of individual and combined toxicities of metals in aqueous samples. In *Handbook on Cyanobacteria: Biochemistry, Biotechnology and Applications* (P. M. Gault and H. J. Marler, Eds.), pp. 283–304. Nova Science Publishers, New York, NY.

Rodea-Palomares, I., González-García, C., Leganés, F., and Fernández-Piñas, F. (2009b). Effect of pH, EDTA, and anions on heavy metal toxicity toward a bioluminescent cyanobacterial bioreporter. *Arch. Environ. Contam. Toxicol.* **57,** 477–487.

Rodea-Palomares, I., Petre, A. L., Boltes, K., Leganés, F., Perdigón-Melón, J. A., Rosal, R., and Fernández-Piñas, F. (2010). Application of the combination index (CI)–isobologram equation to study the toxicological interactions of lipid regulators in two aquatic bioluminescent organisms. *Water Res.* **44,** 427–438.

Rogers, N. J., Franklin, N. M., Apte, S. C., Batley, G. E., Angel, B. M., Lead, J. R., and Belousha, M. (2010). Physico-chemical behaviour and algal toxicity of nanoparticulate CeO_2 in freshwater. *Environ. Chem.* **7,** 50–60.

Roh, J. Y., Park, Y. K., and Choi, J. (2010). Ecotoxicological investigation of CeO_2 and TiO_2 nanoparticles on the soil nematode *Caenorhabditis elegans* using gene expression, growth, fertility, and survival as endpoints. *Environ. Toxicol. Pharmacol.* **29,** 167–172.

Rouquerol, J., Avnir, D., Fairbridge, C. W., Everett, D. H., Haynes, J. H., Pernicone, N., and Ramsay, J. D. F. (1994). Recommendations for the characterization of porous solids. *Pure Appl. Chem.* **66,** 1739–1758.

Thill, A., Zeyons, O., Spalla, O., Chauvat, F., Rose, J., Auffan, M., and Flank, A. M. (2006). Cytotoxicity of CeO_2 nanoparticles for *Escherichia coli*. Physico-chemical insight of the cytotoxicity mechanism. *Environ. Sci. Technol.* **40,** 6151–6156.

Tiede, K., Hassellöv, M., Breitbarth, E., Chaudhry, Q., and Boxall, A. B. A. (2009). Considerations for environmental fate and ecotoxicity testing to support environmental risk assessments for engineered nanoparticles. *J. Chromatogr. A* **1216,** 503–509.

Van Hoecke, K., Quik, J. T., Mankiewicz-Boczek, J., De Schamphelaere, K. A., Elsaesser, A., Van der Meeren, P., Barnes, C., McKerr, G., Howard, C. V., Van de Meent, D., *et al*. (2009). Fate and effects of CeO_2 nanoparticles in aquatic ecotoxicity tests. *Environ. Sci. Technol.* **43,** 4537–4546.

Wilhelm, C., Billotey, C., Roger, J., Pons, J. N., Bacri, J. C., and Gazeau, F. (2003). Intracellular uptake of anionic superparamagnetic nanoparticles as a function of their surface coating. *Biomaterials* **24,** 1001–1011.

Xia, T., Kovochich, M., Liong, M., Mädler, L., Gilbert, B., Shi, H., Yeh, J. I., Zink, J. I., and Nel, A. E. (2008). Comparison of the mechanism of toxicity of zinc oxide and cerium oxide nanoparticles based on dissolution and oxidative stress properties. *ACS Nano* **28,** 2121–2134.

‘, O., Thill, A., Chauvat, F., Menguy, N., Cassier-Chauvatb, C., Oreacutear, C., Daraspe, J., Auffan, M., Rose, J., and Spalla, O. (2009). Direct and indirect CeO_2 nanoparticles toxicity for *Escherichia coli* and *Synechocystis*. *Nanotoxicology* **3,** 284–295.